Microscopic Models for Ultrafast Photoinduced Solvent to Dye Electron Transfer in DMA/Oxazine Solution

P. O. J. Scherer*

Theoretical Molecular Physics T38, TU München D-85748 Garching, Germany

Received: February 22, 2000; In Final Form: April 27, 2000

A microscopic model for the ultrafast photoinduced electron-transfer process in solutions of oxazine-1 in *N*,*N*-dimethylaniline (DMA) is presented. Translational and rotational motions of the solvent molecules are treated classically by molecular dynamics simulations. Along the trajectory, the energy gaps between the optical excitation and the charge transfer states involving the first solvation shell are calculated quantum mechanically, together with the corresponding electron-transfer matrix elements. The first solvation shell consists of ∼20 DMA molecules and is rather stable with a decay time of ∼20 ps. The calculated fluctuations of energy gaps and couplings occur on a time scale of about 0.3−1 ps, considerably slower than the fastest experimentally observed decay time of 70 fs. At most points along the trajectory, at least one DMA molecule is in a position and orientation that gives large electron transfer matrix elements up to 0.08 eV. The coupling of the electron transfer to intermolecular vibrations is investigated with a quantum chemical approach combining ab initio normal modes of the individual molecules and semiempirical electronic structure calculations. Several modes of electron acceptor and donor are identified that act efficiently as accepting modes.

1. Introduction

Ultrafast electron transfer from the solvent *N*,*N*-dimethylaniline (DMA) to an optically excited oxazine (Ox) molecule has been reported to take place on a time scale of less than 100 fs, faster than the solvation dynamics.[1−4] The coherence of the vibrational motions persists much longer (1 ps), and the observed beating phenomena have been attributed to strongly coupling internal vibrations of the oxazine molecule, which are also prominent in its absorption and Raman spectra.[3−4] The observed nonexponential electron-transfer dynamics were explained by a distribution of coupling matrix elements due to the heterogeneity of the DMA molecules surrounding the electron accepting Ox[2].

Little is known about the electron transfer coupling matrix elements, especially their dependence on arrangement and thermal motion of the molecules. As the relative orientation and distance of the electron donor and acceptor fluctuate, the coupling matrix element also changes in time, and the Condon approximation of constant electronic coupling becomes questionable. Furthermore, there may be multiple reaction channels, as the first solvation shell contains a large number (typically 20) of possible electron donors.

In this paper, we apply a combined MD/QM approach to present a model of the DMA/Ox system. Translational and rotational motions are treated classically by a simulation of rigid rotors. This treatment is motivated by the Born−Oppenheimer approximation but is also further justified by the efficient decoherence of molecular motion due to interaction with the surroundings.[5] The spatial extent and stability of the first solvent shell are investigated.

Along a trajectory, semiempirical calculations of the INDO/S type[6] are performed to evaluate the time evolution of the semiclassical Hamiltonian matrix, i.e., the energy gaps between the optically excited-state Ox* and the CT states $DMA_n \rightarrow Ox$, as well as the corresponding electronic coupling matrix elements $V(Ox^*, DMA_n \rightarrow Ox)$.

Finally, we investigate the coupling of internal vibrations to the optical excitation and the CT states. From INDO/S calculations along the normal modes of a donor−acceptor pair, the vibronic coupling parameters are estimated. Intramolecular vibrations that can act efficiently as accepting modes by modulating the energy gap between the optically excited and the final charge transfer state or that influence the electron-transfer coupling are identified.

A classical simulation of all of the nuclear motions would be rather complicated for such large molecules, as the force field must be chosen in such a way that the equilibrium structures and the normal modes are consistent with a quantum calculation. Therefore, we prefer to treat the vibrations separately, retaining their full quantum nature. Our results on vibronic couplings, transfer matrix elements, and energy gaps provide a solid basis for the application of simplified models for the electron transfer that only make use of these parameters and do not involve the detailed structure of the system on an atomic level.

2. Approximations to the Molecular Hamiltonian

A full quantum mechanical treatment of the electron transfer process is impossible because of the large number of degrees of freedom. At least those solvent molecules donating an electron to the oxazine must be treated explicitly. Even the simplest QM/MM model, treating only one donor−acceptor pair explicitly, must cope with 70 atoms and 204 vibrations. Such a model, however, cannot properly deal with the effect of multiple reaction channels and fluctuating transfer couplings. A more realistic model including the first solvation layer explicitly contains ∼500 atoms and around 1500 vibrational modes.

* To whom correspondence should be addressed. E-mail: philipp.scherer@physik.tu-muenchen.de

10.1021/jp0006983 CCC: $19.00
Published on Web 06/13/2000

Therefore, one must reduce the complexity by making suitable approximations. A semiclassical description of the vibrational coherence in photoinduced reactions, based on a generalized Landau Zener treatment, has been presented by Zhu et al..[7] However, for larger values of the electronic coupling, the application of the golden rule becomes questionable, and more complicated theoretical methods are necessary[8,9]

A recent investigation of the DMA/oxazine system[4] uses a quantum mechanical model with two explicit modes representing the internal vibrations of the oxazine around 600 and 1350 cm^{-1}, which are also prominent in the absorption and resonance Raman spectra. The parameters of the model are fitted to reproduce the experimentally observed optical transients. This model, however does not involve optically inactive modes of the oxazine and the solvent that can be essential for the electron transfer as accepting modes.

In this paper, we want to obtain more detailed information about the relevant modes of the system. The slowest degrees are treated classically, and the internal vibrations are considered on a quantum mechanical basis.

To this end, we formally introduce a double separation of time scales. We start from a Born−Oppenheimer like Ansatz for the wave function of the supermolecular system

$$\Psi = \varphi(r_{\mathrm{el}};R,Q)\Phi(R;Q)\chi(Q) \tag{1}$$

involving electronic coordinates (r_{el}), internal nuclear modes (R) such as vibrations and methyl group rotations and as the slowest coordinates (Q), the center of mass position vectors r_m, and the orientations of the molecules, which will be described by orthogonal matrixes A_m transforming from a body fixed to the laboratory coordinate system (see below).

The rotational and translational motion is approximated by a classical trajectory $Q_{\mathrm{cl}}(t) = \{r_m, A_m\}$. Then, the explicitly time dependent semiclassical Hamiltonian reads

$$H = \sum_{s,s',n,n'} |n,s > h_{ns,n's'}(Q_{\mathrm{cl}}(t)) < n', s'| \tag{2}$$

where the label s denotes the electronic state, i.e., the optical excitation Ox* or one of the charge transfer states $DMA_n \rightarrow$ Ox, and n summarizes the state of the intramolecular modes.

We neglect the influence of intermolecular interaction on the intramolecular vibrations, assuming that the internal normal modes are time independent.

Finally, we apply the Franck−Condon approximation for the intramolecular vibrations. Then the diagonal elements of the interaction matrix

$$h_{ns,ns}(Q_{\mathrm{cl}}(t)) = E_{\mathrm{s}}(t) + E_{\mathrm{ns}} \tag{3}$$

are the sum of a fluctuating electronic energy $E_{\mathrm{s}}(t)$ and a time independent vibrational contribution E_{ns}. For simplicity, we neglect a possible change of the normal frequencies going from the neutral to the charged state of a molecule and consider only the shift of the equilibrium positions. Within this approximation, the vibrational energy is the sum of the vibrational quanta and the total reorganization energy of state s

$$E_{ns} = \sum_j n_j\hbar\omega_j - \sum_j S_{\mathrm{js}} \tag{4}$$

Our calculations showed that the energy shifts S_{js} are essentially properties of the isolated molecules and do not significantly depend on intermolecular interactions. This allows further simplification of eq 4

$$E_{n,\mathrm{Ox}^*} = \sum_j n_j\hbar\omega_j - S_{\mathrm{Ox}\rightarrow\mathrm{Ox}^*}$$

$$E_{n,\mathrm{DMA}\rightarrow\mathrm{Ox}} = \sum_j n_j\hbar\omega_j - S_{\mathrm{Ox}^*\rightarrow(0)} - S_{\mathrm{DMA}\rightarrow\mathrm{DMA}+} \tag{5}$$

introducing the reorganization energies of the optically excited oxazine Ox*, its neutral radical $Ox^{(0)}$, and the DMA cationic radical DMA^+.

The nondiagonal element $\boldsymbol{h}_{ns,n's'}(\boldsymbol{Q}_{\mathrm{cl}}(t))$ represents the matrix elements for electron transfer.

Expanding it as a function of the normal coordinates around the groundstate geometries, we have

$$h_{ns,n's'}(Q_{\mathrm{cl}}(t)) = V_{s,s'}(t)\,\mathrm{FC}_{ns,n's'} + \sum_j \frac{\partial V_{s,s'}}{\partial R_j}(t)\,\langle\Phi_{ns}(R_j;Q_{\mathrm{cl}})|R_j|\Phi_{n's'}(R_j;Q_{\mathrm{cl}})\rangle + \ldots \tag{6}$$

Using the Franck−Condon approximation reduces eq 6 to the first summand, which is the product of a fluctuating electronic matrix element and a time independent Franck−Condon factor

$$\mathrm{FC}_{ns,n's'} = \langle\Phi_{ns}|\Phi_{n's'}\rangle \tag{7}$$

The dependence of V on the internal vibrations will be discussed later. The average of the squared interaction over thermal motion of the coordinate R_j gives

$$\langle|h_{s,s'}|^2\rangle = |V_{s,s'}|^2 + \sum_j|\frac{\partial V_{s,s'}}{\partial R_j}|^2(2n_\omega + 1)R_{j,0}^2 + \cdots \tag{8}$$

with the zero point amplitude

$$R_{j,0} = \sqrt{\frac{\hbar}{2m_j\omega_j}} \tag{9}$$

and the thermal occupation

$$2n_\omega + 1 = \coth\left(\frac{\hbar\omega}{2kT}\right) \tag{10}$$

The higher order terms are only significant if $V(t)$ changes its value considerably over a thermal motion with amplitude

$$R_j^{th} = \sqrt{\frac{\hbar}{2m_j\omega_j}\coth\left(\frac{\hbar\omega}{2kT}\right)} \tag{11}$$

of a normal mode j, i.e., if $R_j^{th}\,{}^{\partial V_{ss'}}\!/_{\partial R_j}$ is comparable to or even larger than $V_{ss'}$ For the DMA/Ox system, our calculations generally gave only a minor dependence of V on the internal vibrations, with the exception of some very low-frequency modes.

3. Methods

3.1. Translational and Rotational motion. We simulated one oxazine molecule embedded in a cluster of 125 DMA molecules in a cube of 28 Å length, representing the density of liquid DMA at room temperature. The molecules were kept within the box by reflecting boundaries, i.e., whenever a molecule traversed a boundary, its velocity vector was reversed. This kind of boundary condition proved to be quite useful as it conservesd the kinetic energy and did not introduce Coulombic

repulsion between the charged dye molecule and its mirror images, as in the case of periodic boundaries. The Cartesian coordinate vector of an atom i within molecule m is given in terms of the center of mass position r_m, the coordinates in the body fixed coordinate system $\rho_i^{(b)}$, and an orthogonal rotation matrix A_m as

$$\rho_i = r_m + A_m \rho_i^{(b)} \tag{12}$$

The center of mass motion is calculated by a standard leapfrog algorithm[10]

$$v_m\left(t+\frac{\Delta t}{2}\right) = v_{\mathrm{m}}\left(t-\frac{\Delta t}{2}\right) + \Delta t \sum_{n\neq m} \frac{F_{mn}(t)}{m_m} + \mathrm{O}(\Delta t^3)$$

$$r_m(t+\Delta t) = r_m(t) + v_m\left(t+\frac{\Delta t}{2}\right)\mathrm{d}t + \mathrm{O}(\Delta t^3)$$

$$F_{mn} = \sum_{i\in m,\, j\in n} F(\rho_i - \rho_j) \tag{13}$$

The intermolecular forces $F(\rho_i - \rho_j)$ are derived from a force field combined of a Lennard−Jones term[10] and the Coulombic interaction of point charges at the atom positions ρ_i, which are fitted to the electrostatic potential from a DFT calculation using the DGauss program package.

Several proposals have been made in the literature to implement a leapfrog analogon for rotational motion.[10−14] In contrast to translational motion (eq 13), here, some of the variables must be calculated at midtime steps by interpolation or by solving nonlinear equations iteratively.

In our present investigation, the total integration time is limited by the subsequent quantum calculations and by the lifetime of the first solvation shell to some 10 ps using a time step of 1 fs. We found that a simple integration method is sufficient for our purposes which is based on an algorithm suggested in ref 13.

The orientation of molecule m is described by an orthogonal 3×3 matrix, which transforms from a body fixed coordinate system to the laboratory system. It obeys the equation of motion

$$\frac{\partial A_{\mathrm{m}}}{\partial t} = A_m W_m \quad W_m = \begin{bmatrix} 0 & -\omega_{mz} & \omega_{my} \\ \omega_{mz} & 0 & -\omega_{mx} \\ -\omega_{my} & \omega_{mx} & 0 \end{bmatrix} \tag{14}$$

where W_m is an antisymmetric tensor that is equivalent to the angular velocity vector in the body fixed system. The change of A_m during the time step Δt is approximated by the first terms of the Taylor series

$$A_m(t+\Delta t) = A_m(t) + A_m(t) W_m(t)\Delta t + A_m(t)\left(W_m{}^2(t) + \frac{\partial W_m(t)}{\partial t}\right)\frac{\Delta t^2}{2} + \mathrm{O}(\Delta t^3) \tag{15}$$

and angular velocities and accelerations are calculated from

$$\omega_m(t) = \Theta_m{}^{-1} \mathrm{A}_m(t) L_m(t)$$

$$\frac{\partial \omega_m}{\partial t}(t) = \Theta_m{}^{-1}\left(\frac{\partial \mathrm{A}_m(t)}{\partial t} L_{\mathrm{m}}(t) + A_{\mathrm{m}}(t)\frac{\partial L_m(t)}{\partial t}\right) \tag{16}$$

Θ_m is the tensor of moments of inertia in the body fixed system of molecule m, which is assumed to be diagonal and time independent.

We do not make use of constraints to keep the matrixes A_m orthogonal[13,14]. Instead, each matrix is reorthogonalized whenever its determinant deviates from unity by more than 10^{-5}.

Finally, the change of the molecular angular momentum

$$L_m = \sum_{i\in m} m_{\mathrm{i}}(\rho_i - r_m) \times (\dot{\rho}_i - v_m) \tag{17}$$

is approximated by

$$L_m(t+\Delta t) = L_m(t) + \sum_{n\neq m} M_{mn}\left(t+\frac{\Delta t}{2}\right)\Delta t + \mathrm{O}(\Delta t^3) = L_m(t) + \sum_{n\neq m} \frac{M_{mn}(t) + M_{mn}(t+\Delta t)}{2} + \mathrm{O}(\Delta t^3)$$

$$M_{mn} = \sum_{i\in m, j\in m} (\rho_i - r_m) \times F(\rho_i - \rho_j) \tag{18}$$

Initially, the molecules are placed with random orientations on a grid but using an energy criterion to avoid too close contacts. Velocities and angular velocities are assigned by a thermal distribution and rescaled during an equilibration run to establish a temperature of 300 K. After further 50 ps simulation, a 10 ps trajectory is taken for the subsequent quantum calculations.

3.2. Electron-Transfer Couplings and Charge Transfer State Energies. We investigated the electronic structure of the oxazine and its first solvation shell as a supermolecule. More of the solvent molecules could be taken into account explicitly, but to save computing time, we selected only those 24 DMA molecules that had close contacts to the oxazine within the 10 ps time window that we investigated. The quantum calculations with 10 fs resolution took about two weeks of CPU time on a Silicon Graphics R10000 processor.

As such a large number of excited-state calculations on a system of 500 atoms was not affordable with ab initio methods, we used a semiempirical program that is based on Zerner's INDO/S Hamiltonian, which was parametrized for excited-state calculations.[6]

As our system consists of distinct molecular units, the interacting diabatic states can be generated very easily by localizing the orbitals of the supermolecule on one of the molecular units. This is done by partitioning the one electron part of the INDO Hamiltonian into an intermolecular and an intramolecular part and rearranging the Hamiltonian in the following way.[15]

$$H = \sum_{i,j,\sigma} t_{i,j} a_{i\sigma}^{+} a_{j\sigma} + \sum_{\substack{ijkl \\ \sigma,\sigma'}} V_{ijkl} a_{i\sigma}^{+} a_{k\sigma'}^{+} a_{l\sigma'} a_{j\sigma} = \sum_{m} \sum_{\substack{i,j\in m \\ \sigma}} t_{i,j}{}^{\mathrm{intra}} a_{i\sigma}^{+} a_{j\sigma} + \sum_{\substack{ijkl \\ \sigma,\sigma'}} V_{ijkl} a_{i\sigma}^{+} a_{k\sigma'}^{+} a_{l\sigma'} a_{j\sigma} + \sum_{m\neq n} \sum_{\substack{i\in m \\ j\in m \\ \sigma}} t_{i,j}{}^{\mathrm{inter}} a_{i\sigma}{}^{+} a_{j\sigma} \tag{19}$$

The first two contributions are treated with the conventional Hartree−Fock /CI method and the last summand defines the electron-transfer interaction, which couples the CI states. We like to emphasize that this treatment does not involve any additional approximations to the Hamiltonian itself. For the SCF part of the calculation, all intermolecular resonance integrals $t_{i,j}{}^{\mathrm{inter}}$ between atomic orbitals i,j on different molecules m,n are switched off. As an immediate consequence, the resulting

molecular orbitals are fully localized on one of the molecules. A subsequent CI-singles calculation, based on these orbitals, gives excited states that are either localized on one molecule, like the optically excited state Ox*, or pure charge transfer states, especially the final states $Ox^oDMA_n^+$. Within the zero differential overlap (ZDO) approximation, these charge-transfer states have zero intensity, and the local excitations have no dipole moment admixture from the charge transfer states. Therefore, these states are quite analogous to those used in calculations on covalently linked systems.[16]

The electronic coupling matrix element for transfer of an electron from DMA_k to the oxazine is calculated as the matrix element of the intermolecular resonance interaction between the corresponding CI states.

$$V_k = \langle \mathrm{Ox}^* | \sum_{\substack{i\in \mathrm{Ox} \\ j\in \mathrm{DMAk} \\ \sigma}} t_{ij}^{\ \mathrm{inter}} a_{i\sigma}^{+} a_{j\sigma} | \mathrm{Ox}^o\mathrm{DMA}_k^+ \rangle \qquad (20)$$

3.3. Coupling to Intramolecular Vibrations. The calculation of the vibrational couplings is the most time-consuming part of our calculations. Therefore only one molecular configuration was investigated. Most of the normal modes influence either the donor or the acceptor molecule, and the calculated reorganization energies do not depend on the relative orientation of the molecules.

The situation is different for the derivatives of the transfer matrix elements. However, our results showed that, with the exception of a few very low-frequency (<kT) modes, the transfer matrix element changes only some percents over the zero point motions. The thermally occupied low-frequency modes modulate the donor acceptor distance and orientation on a time scale comparable to translations and rotations. They will be adressed in more detail in a forthcoming paper in which they are included into the set of classical coordinates.

We selected a donor−acceptor pair in a configuration favorable for the ET process. Normal modes for both molecules were separately calculated using the Gaussian program package on the Cray T90 of the Leibniz Rechenzentrum, München. For each of the normal modes, an excitation of zero point amplitude $\pm R_n$ (o) was made and the electronic spectrum calculated.

Within the harmonic oscillator approximation, the energy shifts are calculated from

$$S_{js} = \frac{1}{\hbar\omega_j}\left[\frac{(E_s(R_j^{(o)}) - E_0(R_j^{(o)})) - (E_s(-R_j^{(o)}) - E_0(-R_j^{(o)}))}{2}\right]^2 \qquad (21)$$

and the zero point variation of the matrix element (eq 8) from

$$R_j\frac{\partial V_n}{\partial R_j} = \frac{V_n(R_j^{(o)}) - V_n(-R_j^{(o)})}{2} \qquad (22)$$

4. Results

4.1. Size and Stability of the First Solvation Shell. Figure 1 shows a histogram of the closest contact distances between the oxazine and the solvent molecules. The first solvation shell consists of an average number of 20 molecules with contact distances of 2.5 ± 0.5 Å. Further solvation layers with contact distances of >5.0 are not so clearly distinguishable. Direct electron transfer from the outer layers to the oxazine is unlikely due to the large distances and the exponential distance dependence of transfer coupling matrix elements. In summary, we have to consider ∼20 possible electron donors. The first solvation shell is rather stable. Assuming an exponential time dependence for the number of molecules remaining in the first shell, we estimate a time constant of ∼25 ps.

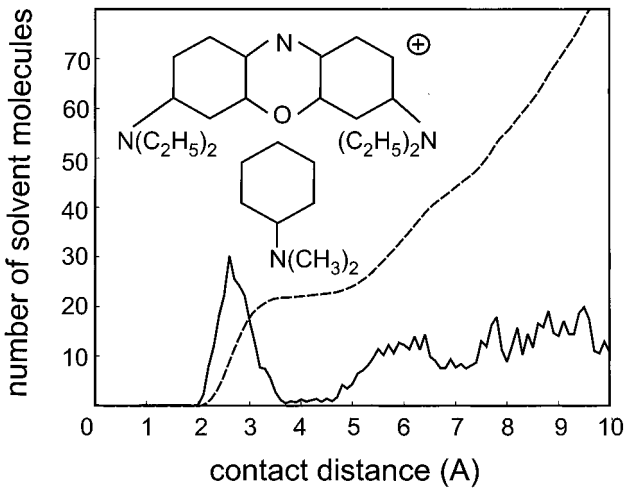

Figure 1. Histogram of the closest atom−atom distances between the central oxazine and the surrounding DMA molecules (full line) and the corresponding integrated distribution function (broken line). Also shown are the molecular structures of oxazine-1 and the solvent DMA

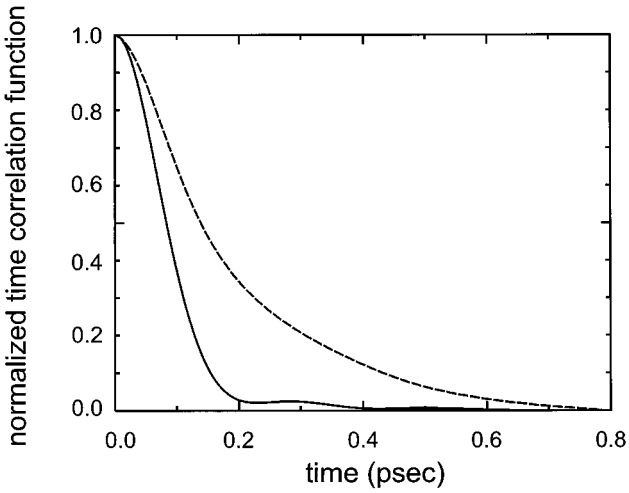

Figure 2. Normalized time-correlation function of the angular velocities (full line) and of the center of mass velocities (broken line).

4.2. Solvent Dynamics. The shortest time scale of our MD simulations relates to the correlation times of velocities and angular velocities (see Figure 2). The time correlation function (TCF) of the angular velocities

$$C_\omega(t) = \langle \vec{\omega}(t_0)\vec{w}(t_0 + t)\rangle \qquad (23)$$

is dominated by an initial Gaussian decay

$$C_\omega^{in}(t) = \langle\omega^2\rangle \exp\left(-\frac{\omega_R^{\ 2}t^2}{2}\right) \qquad (24)$$

with a characteristic frequency of $\omega_R = 10\ \mathrm{ps}^{-1}$. At times $t >$ 100 fs a small oscillatory contribution is observed, which is characteristic for damped rotational motion.[17]

The velocity TCF of the translational motion(see Figure 2) decays somewhat more slowly within about 200 fs.

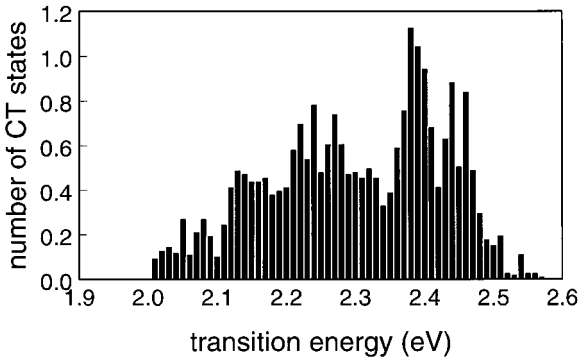

Figure 3. Distribution of calculated transition energies for charge-transfer states from the first solvation layer to the oxazine

Reorientation of the molecules takes place on a much longer time scale. From a rigid body MD simulation of pure DMA, we calculated the normalized correlation functions of the molecular orientation

$$C_i^{(1)}(t) = \langle \vec{e}_i(0)\, \vec{e}_i(t) \rangle \; ; \; i = x, y, z \qquad (25)$$

where $\vec{e}_i(t)$ are unit vectors defining the body fixed coordinate system of a molecule.

Initially, theses TCF's decay with a time constant of 6.5 ps. After few ps, a slower component becomes dominant, with time constants of 9, 11, and 18 ps for the *x*, *y*, and *z* axis, respectively.

The experimental data give comparable pairs of relaxation times. They are 2.8 and 33 ps, determined by optical Kerr effect, and 3.8 and 24.6 ps, determined by dynamic Stokes shift measurements[2]. However, a direct comparison is not straightforward, as the experiments also involve higher order correlation functions (e.g., of the polarizability tensor) and cooperative effects that may be lacking in our finite size model system.

4.3. Fluctuations of Energy Gaps and Transfer Matrix Elements. For the 631G(s,p) optimized structure of the isolated oxazine, we calculated a vertical transition energy of 2.26 eV of the optical excitation. The experimental position of the absorption maximum is solvent dependent. For the nonpolar solvent cyclohexan, it is found at 1.93 eV. From the approximate mirror symmetry of absorption and emission spectra, we expect the vertical $S_0 \rightarrow S_1$ transition to be about 0.03 eV below the absorption maximum. Extrapolating from the dependence on dielectric constant and refractive index,[19] we estimate a vacuum transition energy of 2.07 eV. The excitation energy of the charge transfer state is at large donor−acceptor distances, approximately given by the difference of the orbital energies of the highest occupied orbital (HOMO) of the oxazine and the lowest unoccupied orbital (LUMO) of the DMA. Within the INDO approximation, we calculated an energy difference of 2.13 eV, quite close to the optical excitation of the oxazine. At closer distances electrostatic interactions with the positively charged oxazine together with mutual polarization effects influence the positions of the charge transfer states. The calculated charge transfer states involving solvent molecules of the first shell form a band of 0.5 eV width around the optical transition of the oxazine (see Figure 3). Interactions with more distant solvent molecules are less important. We estimated them by including the remaining atomic charges in the simulated box and the reaction field of a surrounding dielectric continuum. Essentially, all of the charge transfer states were shifted up by 0.1 eV. The optical transition of the oxazine was not affected. The importance of such long-range effects for the solvent relaxation after electron transfer will be investigated in a following publication. Preliminary investigations of the solvent relaxation after a sudden change of the charge distribution simulating the electron transfer gave a stabilization by about 0.1 eV with a relaxation time around 1ps. This can be understood by considering the smaller ion radius of the DMA as compared to the oxazine cation. Using the standard continuum model, a comparable solvent reorganization energy of 0.17 eV was estimated[2]. However, applicability of the continuum model becomes questionable for a donor−acceptor pair in close contact, and the ion radii are not well-defined quantities for nonspherical molecules.

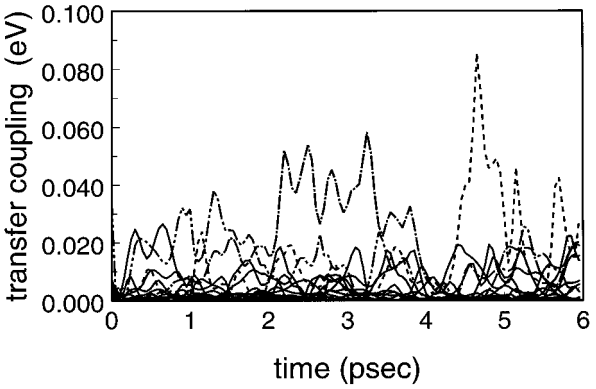

Figure 4. Fluctuation of the electronic coupling matrix elements with time. Only the solvent molecules of the first solvation layer are considered. Individual donor molecules are distinguished by different line types

In the following, we concentrate on the interactions with the first solvation shell only. The optical transition energy is hardly affected by the solvent dynamics, whereas the charge transfer state energies show fluctuations with a correlation time of about 1 ps and an average time derivative of $\sqrt{\langle \dot{E}^2 \rangle} = 0.14$ eV/psec. The estimated frequency of crossings of the optical excitation and one of the CT states is $\leq$ 1/ps, i.e., the solvent motion can be considered frozen, at least for the faster components of the electron-transfer dynamics. The width of a single CT state of $\sqrt{\delta E^2} = \sqrt{\langle (E - \langle E \rangle)^2 \rangle} = 0.04$ eV is small compared to the whole band of CT states reflecting the stability of the first solvation shell on the 10 ps time scale. The normalized energy gap TCF is approximately related to the velocity TCF by[18,19]

$$C_{\Delta E}(t) \cong \exp\left\{ -\frac{\langle \dot{E}^2 \rangle}{\langle \delta E^2 \rangle} \int_0^t dt' (t' - \tau) \frac{2}{3} C_\omega(\tau) \right\} \approx \exp\left\{ -\frac{t}{\omega_R} \frac{\sqrt{2\pi}}{3} \frac{< \dot{E}^2 >}{< \delta E^2 >} \right\} \qquad (26)$$

and again the estimated time constant of 1.2 ps agrees well with the simulations.

Figure 4 shows the fluctuations of the couplings during the 6 ps time window. At most times, one or more of the solvent molecules are good candidates for the electron transfer with large couplings up to 0.1 eV. On the other hand, there are some time intervals in which the maximum couplings are much smaller. The fluctuations of the couplings are somewhat faster than that of the energy gaps with a mean correlation time of 0.35 ps. The coupling values are distributed over a wide range. Figure 5 shows a histogram of the sum of the squared couplings to the first shell as a measure of the overall coupling strength. Within the simulated 6 ps, the minimum value of $\sqrt{\sum V_n^2}$ is 65 cm^{-1}, the maximum value is 800 cm^{-1}, and the average is 300 cm^{-1}.

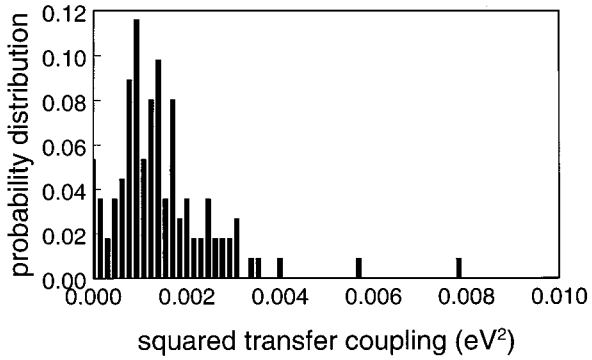

Figure 5. Histogram of the squared couplings. The sum of the squared transfer matrix elements to the first solvation layer is analyzed as a measure of the overall electron-transfer coupling.

4.4. Intramolecular Vibrations. The calculated results for the Oxazine modes are shown in Figure 6. Several modes below 1000 cm^{-1} are strongly coupled to the optical transition of the oxazine. The largest shifts are calculated for a pair of vibrations at 620 cm^{-1} summing up to 0.007 eV and another vibration at 660 cm^{-1} with comparable shift. These frequencies compare quite well with the positions of the two most prominent bands in the resonance Raman spectrum at 567 and 608 cm^{-1}[13]. An earlier simulation of the oxazine absorption spectrum[20] made use of two vibronic progressions of modes at 612 and 1375 cm^{-1} with reorganization energies of 0.03 and 0.07 eV, respectively. These numbers compare reasonably well with the present results. The sum of the reorganization energies is 0.02 eV for the modes below 1000 cm^{-1} as well as for the higher modes. Taking into account the approximative character of the INDO calculations agreement is quite satisfying.

The modes around 600 cm^{-1} are also coupled to the charge-transfer transition with a total shift of 0.03 eV. In addition, three low-frequency modes at 32, 66, and 280 cm^{-1} are predicted to be efficient energy acceptors. In particular, the lowest vibration at 32 cm^{-1} has a calculated reorganization energy of 0.08 eV.

The calculated total reorganization energy contribution of the oxazine modes is 0.28 eV. AM1 calculations by Rubtsov et al. gave a comparable value of 0.2 eV^2. For the solvent contribution, we calculate a larger value of 0.7 eV. It seems unlikely that the INDO approximation leads to an overestimation because a direct ab initio geometry optimization of the DMA^+ cation (6311G-(s,p) UHF) gave almost the same value. Semiempirical calculations, on the other hand,[2] gave a smaller value of only 0.29 eV. All of these calculations, however, are performed for isolated molecules. Because the relaxation involves appreciable geometry changes, it may be hindered partly in the dense liquid. As shown in Figure 7, we find two accepting modes of the DMA at 200 cm^{-1} and 360 cm^{-1} with large energy shifts of 0.1 eV and 0.24 eV.

5. Discussion

In the conventional picture of electron transfer processes in liquids, the solvent fluctuations play an essential role matching the energy gap of the initial optical excitation and the final charge transfer state. In the oxazine/DMA system, however, the transfer process is faster than the solvent dynamics, which can be characterized by a solvation time around 1 ps and a correlation time of the transfer coupling around 0.3 ps. Hence, the dynamics of rotational and translational motion can be considered as frozen on the time scale of electron transfer with an inhomogeneous distribution of energy gaps and coupling matrix elements. Our simulations show that this does not simply imply a distribution of different energy gaps and couplings for different molecules. The first solvation shell contains a large number of potential electron donors providing a distribution of charge transfer states with different energy gaps and couplings for each oxazine molecule. Some of the solvent molecules are in an orientation that favors electron transfer energetically already before the transfer occurs. This corresponds to the fast component of the dynamics, which must be characterized as a pure intramolecular process in which efficient intramolecular modes take up the excess energy.

Assuming activationless transfer, which seems reasonable for the oxazine/DMA system,[2] we want to make a rough estimate

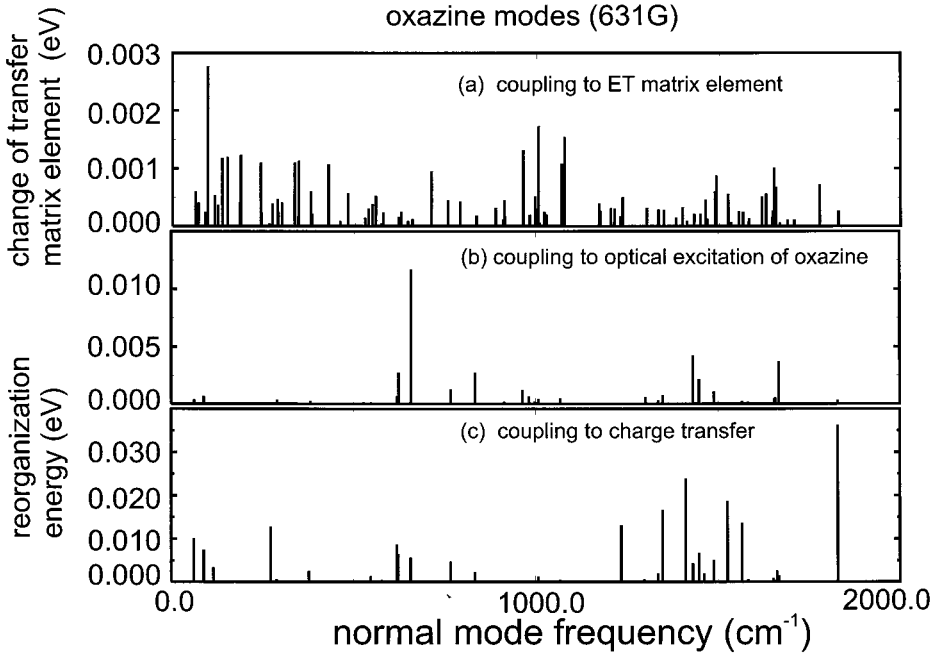

Figure 6. Calculated results for the oxazine modes: (a) zero point variation of the electron-transfer matrix element; (b) reorganization energies of the optical oxazine excitation; and (c) reorganization energies of the charge-transfer transition.

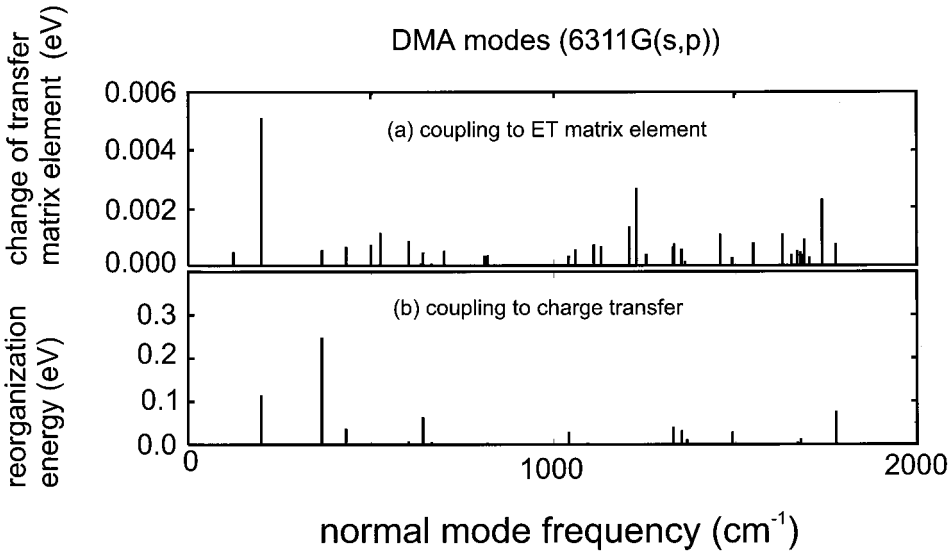

Figure 7. Calculated results for the DMA modes: (a) zero point variation of the electron-transfer matrix element; (b) reorganization energies of the charge-transfer transition.

of the transfer rate applying the standard Golden Rule formula for nonadiabatic transfer[21]

$$k = \frac{2\pi V^2}{\hbar} FCD \tag{27}$$

For the Franck−Condon weighted density of states, we consider contributions of the strongest coupling DMA modes at 200 and 360 cm^{-1} and the prominent oxazine mode at 620 cm^{-1} with estimated Franck−Condon factors of 0.2, 0.1, and 0.4, respectively, and a progression of the lowest oxazine mode with a Franck−Condon factor of 0.1 and a density of $0.03/cm^{-1}$. The estimated overall Franck−Condon weighted density is 2×10^{-5} $/cm^{-1}$. For the maximum electronic coupling of 800 cm^{-1}, the estimated rate is 15 ps^{-1}, which is in the range of the fastest experimentally observed transfer rates. For smaller couplings, the estimated rate can become slower than the solvent dynamics (e.g., for the minimum value of 64 cm^{-1}, the estimated rate is 0.1 ps^{-1}). In this case, the transfer dynamics will depend on the solvent motion that brings the system into a more favorable configuration within about 1ps according to our simulations. A similar behavior has been observed on a longer time scale with single molecule experiments on a related oxazine dye linked to DNA oligonucleotides.[22]

For a detailed description of the transfer dynamics, it will be necessary to consider the influence of fluctuating energy gaps and transfer couplings more explicitly. From calculations that model the fluctuations by simple stochastic processes,[23−25] one has to expect a switch over from simple decay kinetics with an average rate for fast fluctuations to a distribution of rates in the limit of slow fluctuations.

Acknowledgment. The author would like to thank S. Fischer and W. Zinth for stimulating discussions and Christina Scharnagl for reaction field calculations. This work was supported by the Deutsche Forschungsgemeinschaft (SFB 377).

References and Notes

(1) Seel, M.; Engleitner, S.; Zinth, W. *Chem. Phys. Lett.* **1997**, *275*, 363.

(2) Rubtsov, I. V.; Shirota, H.; Yoshihara, K *J. Phys. Chem.* **1999**, *A103*, 1801.

(3) Engleitner, S.; Seel, M.; Zinth, W. *J. Phys. Chem.* **1999**, *A103*, 3013.

(4) Wolfseder, B.; Seidner, L.; Domcke, W.; Stock, G.; Seel, M.; Engleitner, S.; Zinth, W. *Chem. Phys.* **1998**, *233*, 323.

(5) Zeh, H. D. In *Decoherence: Theoretical, Experimental and Conceptual Problems*; Blanchard, Ph. et al., Eds.; Springer: Berlin/ Heidelberg, 2000.

(6) Thompson, M. A.; Zerner, M. C. *J. Am. Chem. Soc.* **1990**, *112*, 7828.

(7) Zhu, L.; Widom, A.; Champion, P. *J. Chem. Phys.* **1997**, *107*, 2859.

(8) Evans, D. G.; Nitzan, A.; Ratner, M. A. *J. Chem. Phys.* **1998**, *108*, 6387.

(9) Schwieters, C. D.; Voth, G. A. *J. Chem. Phys*. **1998**, *108*, 1055.

(10) Allen, M. P.; Tildesley, D. J. *Computer Simulation of Liquids*; Clarendon: Oxford, 1987.

(11) Svaberg, M. *Mol. Phys.* **1997**, *92*, 1085.

(12) Dullweber, A.; Leimkuhler, B.; McLachlan, R. *J. Chem. Phys.* **1997**, 107, 5840

(13) Omelyan, I. P. *Comput. in Phys.* **1998**, *12*, 97.

(14) Omelyan, I. P. *Phys. Rev. E* **1998**, *58*, 1169.

(15) Scherer, P. O. J.; Fischer, S. F. *Spectrochim. Acta* **1998**, *A54*, 1191.

(16) Cave, R. J.; Newton, M. D. *Chem. Phys. Lett.* **1996**, *249*, 15.

(17) Déjardin, P. M. *J. Mol. Liq.* **1999**, *81*, 181.

(18) Ladanyi, B. M.; Maroncelli, M. *J. Chem. Phys.* **1998**, *109*, 3204.

(19) Castner, E. W., Jr.; Maroncelli, M. *J. Mol. Liqu.* **1998**, *77*, 1.

(20) Scherer, P. O. J. Thesis, TU München Physikdepartment: Munich, 1984.

(21) Kavarnos, G. J. *Fundamentals of Photoinduced Electron Transfer*; VCH Publishers: New York, 1993.

(22) Sauer, M.; Drexhage, K. H.; Lieberwirth, U.; Müller, R.; Nord, S.; Zander, C. *Chem. Phys. Lett*. **1998**, *284*, 153.

(23) Frantsuzov, P. A.; Fischer, S. F.; Zharikov, A. A. *Chem. Phys.* **1999**, *241*, 95.

(24) Pudlak, M. *Czech. J. Phys.* **1998**, *48*, 293.

(25) Scherer, P. O. J. *Chem. Phys. Lett.* **1993**, *214*, 149.